Novel Choline-Alginate Hybrid Nanocarrier for Controlled Insulin Delivery

R.Dhandayuthabani[1], M.Syed Muzammil[1], V.Sugantha Kumari[2], S.Khaleel Basha[3,*]

[1]Department of Biochemistry, C.Abdul Hakeem College (Autonomous) Melvisharam – 632 509 Ranipet District (Affiliated to Thiruvalluvar University, Serkkadu, Vellore, TamilNadu, India).

[2]Department of Chemistry, Auxilium College (Autonomous) Vellore – 632 006, Vellore District (Affiliated to Thiruvalluvar University, Serkkadu, Vellore, TamilNadu, India).

[3]Department of Chemistry & Biochemistry, C.Abdul Hakeem College (Autonomous) Melvisharam - 632 509, Ranipet District (Affiliated to Thiruvalluvar University, Serkkadu, Vellore, TamilNadu, India).

Corresponding Author:-

Dr.S.Khaleel Basha

Assistant Professor, Department of Chemistry & Biochemistry, C.Abdul Hakeem College (Autonomous) Melvisharam - 632 509, Ranipet District (Affiliated to Thiruvalluvar University, Serkkadu, Vellore, TamilNadu, India).

Mail id:- khaleel.che@cahc.edu.in

Abstract

An innovative ionic gelation-solvent evaporation method was used to fabricate insulin-loaded Alginate-Lipid Hybrid Nanocomposites (ALHNC) for oral delivery. The incorporation of insulin into ALHNC was validated using Fourier Transform Infrared Spectroscopy (FTIR). Analysis using Transmission Electron Microscopy (TEM) revealed spherical particles with a Polydispersity Index (PDI), a zeta potential of +20.88±1.67 mV, and a uniform diameter of 230 nm. The loading and encapsulation efficiencies were assessed using the HPLC-UV method. Insulin is a pH-responsive substance that releases at higher pH levels and shields it from the harsh gastrointestinal environment, according to in vitro drug release assays conducted in simulated gastric fluid (SGF) and simulated intestinal fluid (SIF). Cytotoxicity studies demonstrated acceptable biocompatibility, while circular dichroism (CD) spectroscopy verified structural stability. The Caco-2 cell model was used to evaluate the apparent permeability (Papp) of insulin-loaded and unloaded ALHNC for intestinal absorption and transmembrane transport. The colon's enterocyte endocytosis was verified using Confocal Laser Scanning Microscopy (CLSM). Male albino rats used in pharmacokinetic investigations demonstrated better mean residence time and half-life with synchronized insulin infusion. ALHNC showed improved absorption and intracellular dispersion in Caco-2 cells. The promise of these nanocomposites as efficient nanocarriers for oral insulin administration is highlighted by their strong mucoadhesive qualities, regulated release, and exceptional stability.

Keywords Diabetes mellitus · Oral drug delivery · Insulin · Nanoalginate synthesis · Nanocomposite.

1. Introduction

It is estimated that 1.3 billion people worldwide will have diabetes by 2050, making it a serious health concern [1]. Ins and other pharmaceutical therapies are essential for controlling blood glucose levels in diabetics. Since hypodermic Ins injections must pass through the skin or mucosal barrier, they can cause dermal trauma and pain, despite their effectiveness due to their ease of administration [2]. Protein and peptide oral drug delivery systems (ODDSs) have garnered a lot of attention lately. Recent advances in biology and nanotechnology have created new opportunities to achieve these objectives. [3] Oral delivery can benefit from a variety of physicochemical and functional characteristics offered by nanocomposite delivery systems, such as liposome surface functionalization [4]. Among them, polysaccharides produced from marine sources, like alginate, have several benefits, such as abundance, broad dispersion and high cytocompatibility, ease of production, biodegradability, and biocompatibility [5].

Effective inhibition of the P-glycoprotein efflux pump, which restricts oral bioavailability via the transcellular pathway, has been demonstrated for alginate [6]. Below about pH 3.5, alginate and peptides (or proteins) are attracted to each other electrostatically [7]. Alginate hydrogel beads, alginate nanoparticles, and alginate microparticles cross-linked by calcium ions have been created to shield protein and peptide medications against enzymatic degradation and low stomach pH levels [8]. The creation of liposomes and micelles commonly uses phosphatidylcholine, a lipid combination made of phospholipids. Notably, these lipid-based nanostructures are made more stable and have mucoadhesive qualities thanks to the alginate covering [9]. Protein encapsulation efficiency is greatly increased by the solid lipid core-shell structure, with the outer lipid shell shielding the encapsulated protein medication from gastrointestinal proteases. This enhances medication stability, allowing for regulated drug release and limiting proteolytic breakdown after administration. In many drug delivery applications, multi-compartmental delivery systems have been used because they provide regulated and sustained release [10]. Solid lipid delivery systems are very promising because of their many advantages over traditional formulations, which include superior physical stability, spherical morphology, uniform size, positive zeta potentials, high cell penetration efficiency, and the use of carbohydrates with generally recognized as safe (GRAS) status [11].

Significant progress in the creation of modified release drug delivery systems has been made possible by the combination of two or more polymeric components. A logical way to produce materials with appropriate biopharmaceutical qualities for drug administration and targeting is to use blends. Controlled drug release is made possible by the solid lipid matrix, which also improves drug stability and guards against proteolytic degradation after injection [12].The outcomes of recent developments in oral Ins delivery have been encouraging. One noteworthy study concentrated on creating a lipid nanocomposite of nanoalginate that responds to pH. For efficient oral Ins delivery, this formulation showed improved encapsulation stability and efficiency in simulated intestinal and stomach fluids [13].

The novel carrier presented in this ground-breaking work has a lipid core that controls and maintains Ins release, together with a mucoadhesive coating that improves Ins retention during the absorption gap. To predict the in vivo effectiveness of the produced nanoalginate in an animal model of diabetes, Ins penetration was also assessed utilizing a variety of cell monolayer experiments. This work represents a masterful combination of state-of-the-art methods to address the mucosal barrier and enzymatic breakdown.

2. Materials and Methods

2.1 Materials

All analytical-grade chemicals were used in our research study. Ethanol, calcium chloride ($CaCl_2$), solid phosphatidylcholine, Span^{TM} 20, sodium alginate (low molecular weight) were purchased from Sigma Aldrich. Insulin, Biphasic isophane, (40 I.U/ml, 10 ml), [(Human Mixtard, Monocomponent Biosynthetic r-DNA Ins obtained from Torrent Pharmaceuticals Ltd), (Novo Nordisk India Pvt Ltd)]. Caco-2 (human epithelial colorectal adenocarcinoma cell) was purchased from American Type Culture Collection (ATCC) (Rockville, MD, USA). For all the experiments, milli-Q water was used. All other chemicals used were of Good and Analytical grade.

2.2 Synthesis of Calcium cross-linked Alginate Nanoparticles (AlgNPs)

A modified version of the ionic gelation process was used to create AlgNPs. The first step involved making a 0.3% w/v sodium alginate solution (20.0 mL) and bringing its pH down to about 6.0. 0.5 mL of Span 20 was then added to this solution, and it was stirred for an hour at 60°C to homogenize it. A 22-gauge needle was used to add 20.0 mL of 0.05% w/v $CaCl_2$ solution drop wise to the homogenous mixture while swirling at 1800 rpm in order to cross - link it. The adding rate was regulated with a syringe pump at 1.0 mL per minute. To separate the resulting nanoparticle pellets, the mixture was centrifuged for 30 minutes at 10,000 rpm after being chilled for the entire night, following a milli Q water wash of these pellets, the nanoparticles and supernatants [14].

2.3 Fabrication of Ins-Loaded and Unloaded ALHNC

The production of Ins-loaded and unloaded ALHNC was modified somewhat in accordance with Solairaj D *et al.*, This simple emulsification/evaporation method comprised mixing 800 µL of an Ins solution (150 mg of Ins in 10 mL of 0.2 M phosphate-buffered saline (PBS), pH 7.4, USP 34) with 50 mg of AlgNPs. For half an hour, this mixture was mixed slowly. At the same time, ethanol (25 mg/mL) was used to dissolve 25 mg of phosphatidylcholine, and Span-20 was added as a surfactant. At 800 rpm, this solution was also gently swirled for 30 minutes. After that, different concentration ratios of the components were combined (1:3, 3:1, and 3:3). The ideal ratio of 3:3 was chosen for additional research after 15 minutes of constant stirring produced Ins-loaded ALHNCs [15].

3. Determination of Ins Association Efficiency (AE) and Loading Capacity (LC)

The AE was calculated indirectly by calculating the difference between the total amount of Ins required to make the systems and the amount of Ins left in the aqueous phase after ALHNC was isolated by filtering it through a 0.2 µm filter. (Schleicher and Schuell, Germany) The amount of Ins trapped in ALHNC was measured. An HPLC-UV method that our team had previously developed and verified was used to measure the amount of Ins present in the filtrate. After then, the following formula was used to determine the AE [15].

$$\text{AE } (\%) = \frac{\textit{The total amount of Insulin} - \textit{Amount of free Insulin in the Supernatant}}{\textit{The total amount of Insulin added}} \times 100$$

(LC) is the percentage of ALHNC's total dry mass that makes up the difference between the quantity of free Ins left over after particle separation and the total amount of Ins needed to manufacture ALHNC. To find the dry mass, a sample of hydrated ALHNC that was obtained after isolation was freeze-dried [15].

$$\text{LE } (\%) = \frac{\textit{The total amount of Insulin} - \textit{Amount of free Insulin in the Supernatant}}{\textit{The total amount of Insulin added}} \times 100$$

4. Determination of Ins

An HPLC-UV reversed-phase method was used to measure the amounts of Ins. The HPLC system included a quaternary pump, auto-sampler, degasser, column heater, and tunable UV detector (1100 series, Agilent Technologies, Santa Clara, CA, USA). A C_{18} pre-column (2 mm x 20 mm, Alltech) and a Zorbax C_{18} column (5 µm, 4.6 mm x 150 mm, Agilent) were used for detection at 25°C. Acetonitrile and a 0.57% phosphoric acid solution, adjusted to pH 2.25 using triethylamine, made up the mobile phase in a volume ratio of 26:74. A wavelength of 220 nm and a flow rate of 1.0 mL/min were used for detection [16].

5. Characterization of both Ins Loaded and Unloaded ALHNC

5.1 Size and Surface Morphology Characterization

Laser dynamic light scattering (DLS) was used to estimate the average particle size and polydispersity index (PDI) of the generated ALHNC. The ALHNC solution was diluted to 1/50 v/v in HPLC water in order to conduct the particle size analysis in triplicate. The PDI value indicates the ALHNC particle size distribution in a given sample. Higher PDI values indicate a distribution of ALHNC with a wide range of sizes, which might result in aggregates and lower particle suspension stability and homogeneity [14]. The zeta potential of the ALHNC suspension was evaluated using the Malvern Zetasizer (Malvern, Worcestershire, UK) following a 50-fold dilution with HPLC water. Zeta potential, a measure of particle surface charge, was used to determine the stability of the ALHNC in the suspension [17].

5.2 Stability Study

The ALHNC's physical stability was evaluated by tracking its hydrodynamic diameter, particle size distribution, and surface properties for 30 days at 4°C in suspension. Previously noted EE% and Recovery% experiments were also conducted during this time. In stomach circumstances, ALHNC's physical permanence was tested as follows. An equal volume of simulated stomach fluid (0.32% w/v pepsin, 2 g sodium chloride, and 7 mL HCl dissolved in 1 L water with pH adjusted to 2.0 using 1M HCl) was incubated with 5 mL of ALHNC nanocomposite suspension for two hours at 37°C in a horizontal shaker. Following two more hours of shaking at 37°C, the mixture was supplemented with simulated intestinal fluid (lipase 0.4 mg/mL, bile salts 0.7 mg/mL, pancreatin 0.5 mg/mL, and calcium chloride solution 750 mM at pH 7.0) [18].

5.3 Fourier Transform Infrared Spectroscopy (FTIR) Analysis

In order to determine chemical constituents, molecular structures, and surface characteristics of Ins-loaded and unloaded ALHNC, FTIR spectroscopy (TENSOR 27, Bruker, Germany) was used. In the wavelength range of 400 to 4000 cm^{-1}, the lyophilized formulations of KBr discs were prepared and analyzed [19].

5.4 Transmission Electron Microscopy (TEM) Analysis

The surface morphology of the loaded and unloaded Ins ALHNC was investigated using a transmission electron microscope (JEM-200 CX, JEOL, Tokyo, Japan). The loaded and unloaded Ins ALHNC sample was put on a carbon-laden copper grid, vacuum-dried until completely dry, and then examined. The appropriate images were taken at different magnifications after the excess sample was removed from the grid [13,20].

5.5 Conformational Stability of Ins

Circular Dichroism (CD) Spectroscopy (Jasco J-810, Jasco Corp, Tokyo, Japan) was used to assess Ins's conformational stability. One milliliter of loaded ALHNC was removed by combining 10 milliliters with a pH 1.0 hydrochloric acid solution and 4 milliliters of methanol. Following a 10-minute centrifugation at 16,000 g, the Ins was extracted from the supernatant. They next separated the Ins [20], using a Supelco ENVI-18 solid-phase extraction column (Sigma-Aldrich). In conclusion, a solvent was added to balance the ENVI-18 column after it had been activated with methanol. After that, a combination of 1 mL supernatant was plated. Following the removal of impurities using 3 milliliters of 40% aqueous methanol, 30 milliliters of 60% aqueous methanol were used to elute the Ins. The CD test was performed by raising the Ins concentration to 30 μg/mL using a hydrochloric acid solution. At 20°C, spectra were acquired with a 0.5 nm step size, a maximum wavelength range of 200-300 nm, a 3 nm band width, a scanning speed of 500 nm/minute, and a reaction time of 0.25 s. Version 1.0 of the Jasco w32 secondary structure estimate program was used to calculate the secondary structure content [21].

5.6 In vitro drug release

The feasibility of the suggested administration strategy for peptide and protein oral delivery was assessed by examining the rate and degree of Ins release as a model medication in the SIF pH 1.2, SGF (duodenum) pH 6.8, and PBS pH 7.4 colon pH [22]. The in vitro release of Ins from ALHNC was tested by mixing 30 mg with 500 mL of SIF solution and shaking the mixture at 50 rpm. The mercury stayed at 37°C±5°C. It was intended for the releasing medium to be fairly large in order to reach the sink state. One milliliter aliquots were taken at predetermined intervals and replaced with heated blank medium. The samples were centrifuged for 20 minutes at 14,000 rpm. Rather than adding blank medium after removing the aliquot, the supernatant was examined for Ins. Previously reported HPLC method was used to measure the amount of Ins present in the supernatant. Data on Ins release in vitro was fitted to the Ritger-Peppas equation in order to better understand the peptide release process from the nanoparticulate drug delivery device.

$$\frac{M_t}{M_\infty} = Kt^n$$

The cumulative release of Ins at time (t) is represented by M_t, and at infinite time by M_∞. An exponent representing the diffusion mechanism is 'n', whereas *K* is a constant associated with the geometric and structural characteristics of the device. The release mechanism was determined by counting the computed values for 'n'. The release mechanism is Fickian/case I diffusion if n = 0.45, non-Fickian/anomalous transport if n < 0.89, and diffusion coupled with zero-order (case II) transport if n = 0.89 [17, 22].

5.7 Transepithelial electrical resistance (TEER) and Ins transport studies

The Caco-2 cell lines were cultivated in transmembrane inserts (Millipore) with a pore size of 0.4 μm and a cell density of 5×105 cells/well. Aspart Ins, a novel and short-acting analogue of human Ins, was also loaded in either the plain Ins loaded ALHNC or the without Ins load ALHNC as a blank with the same concentration. Ins's monomeric structure and linear shape in aqueous media give it a greater ability to cross the lumen epithelium.

The TEER of the cell monolayer was measured at predetermined intervals at 37°C using 10 mg/mL/well concentrations of the Ins loaded ALHNC and without Ins loaded ALHNC as a blank. We compared the results of examining aspart Ins and human Ins under the same settings in order to evaluate the donor chamber of the cell layer received a straightforward solution comprising human Ins and aspart Ins as a control. The donor chamber medium was supplemented with fresh medium containing Ins-ALHNC and blank (10 mg/well) for the purpose of Ins transport studies. The Ins content of the samples was measured after aliquots were taken from the receiver chamber at predetermined intervals over the course of four hours. The mean data for each occurrence were given after it was analyzed three times. $P_{app} = (d_Q/d_t)/A$ is the following formula. Using C_0, the apparent permeability coefficient (P_{app}) of Ins was calculated. This equation represents the initial Ins concentration in the apical chamber, C_0, the permeability rate, d_Q/d_t, and the surface area of the filter membrane [23].

$$P_{app} = \frac{\frac{dQ}{dt}}{A \times C_0}$$

5.8 In vitro Cytotoxicity of ALHNC

The Caco-2 cells proliferate in environments with elevated glucose levels. 10% foetal bovine serum, 1% v/v non-essential amino acids, 50 U/mL penicillin, and 50 µg/mL streptomycin are included in Dulbecco's modified Eagle medium. For 21 days, Caco-2 cells were grown in monolayer culture. For the first fifteen days, the culture media was changed every two days, and for the final week, it was changed daily. The cells were cultured at 37°C in 5% CO_2. The MTT assay was performed to evaluate the cytotoxicity of an Ins-loaded ALHNC on Caco-2 cells over the course of 24 hours. In order to enable confocal microscopy imaging, Caco-2 cells ($1x10^5$ cells/well) were cultivated in 6-well plates for duration of 24 hours. Subsequently, sterile glass cover slips were placed over the wells. The cells received 10 µg/mL dosages of Ins-FITC and Ins-FITC loaded ALHNC-Ins at different times. Following a thorough cleaning with PBS pH 7.4, cell monolayers were examined under a confocal microscope (CLSM, Carl Zeiss Microscopy GmbH, Germany). One Caco-2 cell at a time was exposed after planting. The cells were pretreated with a 1 mM folic acid solution to stop receptor-mediated endocytosis. After that, Ins-loaded ALHNC containing 10 µg/mL Ins was applied to the cells for four hours at 37°C. The cells were lysed with 0.1% Triton X-100 after being washed three times with cold PBS. Intracellular Ins absorption was measured without inhibitors using the manufacturer-recommended ELISA kit as a control [24].

6. Statistical Data Analysis

The results' mean and standard deviation were shown. A one-way analysis of variance (ANOVA) was used to compare the groups (SPSS 16.0, IBM Corp, Amonk, NY). A difference was deemed statistically significant if its P-value was less than 0.05.

7. Results and Discussions

7.1 AE and LC

The effectiveness of ALHNC's drug entrapment was assessed while keeping the drug concentration constant using a novel indirect method. It was shown that more than 80 percent of the formulations had high association efficiency when different fat and alginate concentrations were analyzed. At a 3:3 ratio, ALHNC notably showed the highest association efficiency, at 89.2%. The lipid layer is responsible for this notable effectiveness, since it significantly improves drug loading capacity and association efficiency in comparison to conventional polymeric nanoparticles. Recent advances in nanotechnology highlight the significance of lipid layers in improving drug delivery methods for nanoparticles, and the lipid coating on the polymer's exterior offers structural stability and stops hydrophilic medicines from leaking [11].

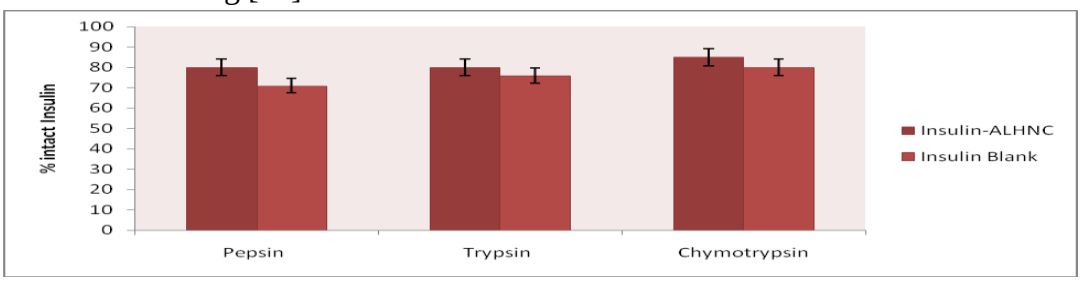

Fig. 1 Effect on Association Efficiency

7.2 Particle Size and Surface Charge

Electrostatic self assembly was used to synthesize ALHNC in a 3:3 ratio, which was simple and dependable. Alginate's ζ-potential was +20.88±1.67 mV, indicating that it retained a positive surface net charge at pH >4.5. At a particular pH, the charge state of polyelectrolytes was ascertained by analyzing the ζ-potential, which represents the electrical potential at the hydrodynamic shear plane in relation to the solvent. Abodinar *et al.*, used ζ-potential measurements to examine the conformation, chain flexibility, and ionic strength dependency of polyelectrolytes in diluted solution. It is not a replacement for potentiometric or conductimetric investigations, and the ζ-potential parameter is sensitive to the structural and conformational properties of polyelectrolytes. Alginate's anionic characteristic decreases below pH 4.4 as a result of carboxylic group dissociation, and its pH dependency is consistent with the known pKa range of 3.4-4.4. Requirements including sufficient encapsulation, high drug encapsulation efficiency, and drug loading efficiency are crucial for oral peptide delivery systems like Ins. Ins absorption across intestinal membranes has been shown for submicron carriers. Smaller, appropriately charged nanocomposites can enter the systemic circulation through the lymphatic system, whereas bigger particles are likely to remain in Peyer's patches and exhibit slower activity. For effective Mcell uptake, nanocomposites should be smaller than 1 μm, or more precisely, smaller than 200 nm. Our study began with reducing the nanocomposite droplets to nanoscale dimensions. The mineral calcium is important for the potential of the nanocomposite to enhance mucosal transport is beneficial. Tight junctions can be opened to compensate for cell shrinkage caused by increased water absorption capabilities of nano alginate [25]. The ability of the nanoalginate-Ins to withstand gastro intestinal enzyme break down is crucial for oral Ins bioavailability. There was no significant variation in particle size or zeta potential in the presence of pepsin, trypsin, or chymotrypsin, and the ALHNC loaded Ins retained more than 75-80% of the encapsulated Ins in the three different biological enzymes. However, more than 78-80% of the naked Ins was destroyed under the same conditions. The ability of the ALHNC loaded Ins to endure harsh gastro intestinal conditions could be attributed to nanoalginate carboxylic/amino groups bonding with Ca^{++}, a recognized cofactor for enzyme function. Finally, the lack of significant changes ($p > 0.05$) in EE%, particle size, and zeta potential at different time intervals and after 6 month storage at 5°C indicated the ALHNC loaded Ins physically durability [26].

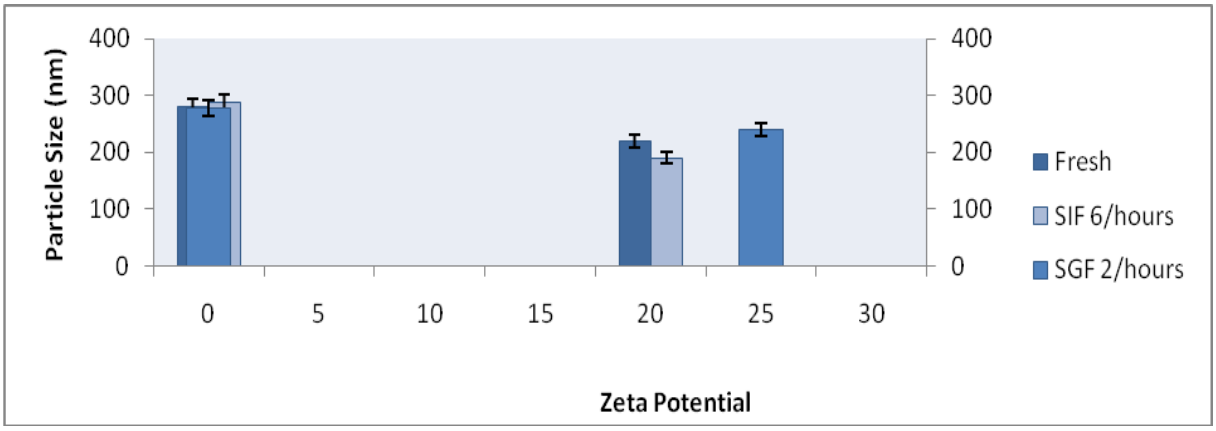

Fig. 2 Effect on Particle Size and Zeta Potential

Table. 1 Physicochemical characterization of Ins-ALHNC

Lipid- Alginate Ratio	Particle size (nm)	PDI	Zeta potential (Mv)	AE (%)	LC (%)
3:3	210± 0.5	0.37± 0.1	+20.05 ±0.10mV	89.5±1.5	1.69±0.5

Results-indicate average Mean±SD n=3, AE-Association efficiency, LC-Loading Capacity.

7.3 Physical stability

Physical stability, dispersion, and particle size are the main determinants of ALHNC's bioavailability. We looked at how these important parameters are affected by factors such Ins peptide concentration, sonication, homogenization, lipid-topolysaccharide ratio, pH, and polydispersity index (PDI). Our goal in adjusting these variables was to maximize the particle size and improve ALHNC's PI and physical stability [26].

7.4 Morphology of the Loaded and Unloaded ALHNC by FTIR

FTIR study clarified how lipids and carbohydrates interacted in ALHNC. Figure 3 shows the FTIR spectra of the nanoparticles as well as those of their constituent lipid and alginate. The major component's distinctive absorption bands of phosphatidylcholine were clearly seen in the spectra. The nanoparticle spectra did not include the alginate band at 1590 cm^{-1}, which is linked to NH_2 scissoring vibrations. This is probably because, in acidic environments, the phosphate groups of phosphatidylcholine and the amino groups of alginate interact ionotically. Nonetheless, the absorption peak of the amino group at 1660 cm^{-1} remained. Furthermore, when fatty acid carbonyl groups were stretched, the absorption band at 1738 cm^{-1} in the nanoparticle spectra was less intense than when phosphatidylcholine was used alone. Ionic interactions between the amino groups of alginate and the phosphate groups of phosphatidylcholine were indicated by the change of the phosphate group absorption band from 1236 cm^{-1} in phosphatidylcholine to 1217 cm^{-1} in the nanoparticle sample. FTIR analysis verified the chemical compatibility of ALHNC components, with physicochemical properties like size, morphology, polydispersity, drug entrapment, and drug content being optimal for oral drug delivery. Cordone *et al.*, reported that polysaccharide coatings significantly reduced mean square fluctuations in polypeptides, resulting in quasi-harmonic behavior at near room temperature [27].

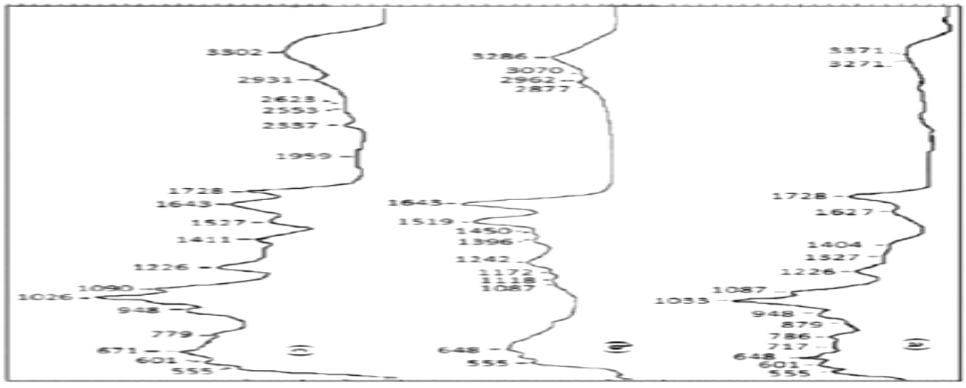

Fig. 3 FTIR Spectrum of (a) Sodium alginate Nanoparticle (b) Insulin (c) ALHNC loaded with insulin

7.5 Morphology of the Ins Loaded and Unloaded ALHNC by TEM

To investigate the morphology of ALHNC with and without Ins, transmission electron microscopy (TEM) was employed [13]. The positive and negative charges inside the hybrid NPs produced an interwoven lipoplex structure in the 230 nm spherical nanoparticles that were visible in TEM images (Fig. 4b, 4c). By obstructing their entry into the system, the lipid coating and lipoplex arrangement seen in the pictures successfully stopped the diffusion of drugs and water. The alginate lipid coating gives the system long-term circulation characteristics [27].

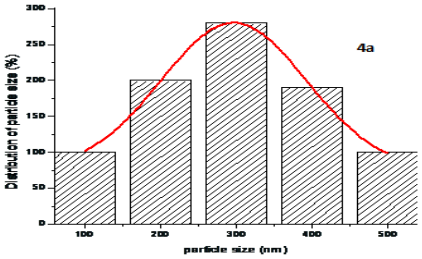

Fig. 4a Histogram of ALHNC

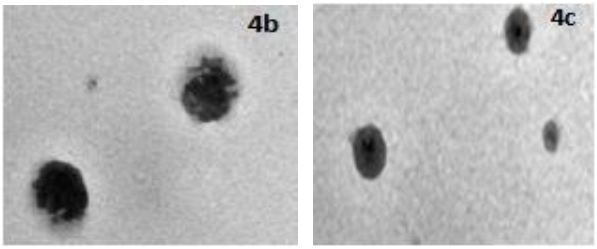

Fig. 4b,c TEM of Ins loaded and unloaded

7.6 Conformational Stability of Ins

The bioavailability of ALHNC is mostly determined by its physical stability, particle size, and dispersion. The effects of factors including pH, calcium-binding efficiency, and polysaccharide-to-lipid ratio on these parameters and the PDI were investigated in our study. In order to maintain therapeutic efficacy, proteins and peptides must be protected from denaturation caused by mechanical manipulation, exposure to organic solvents, and high temperatures. When altering peptides or proteins, it is therefore essential to preserve conformational stability. Ins's potency can be demonstrated with the help of CD Spectra, a reliable method for examining secondary structures in proteins and peptides, including the α-helix and β fold [26].

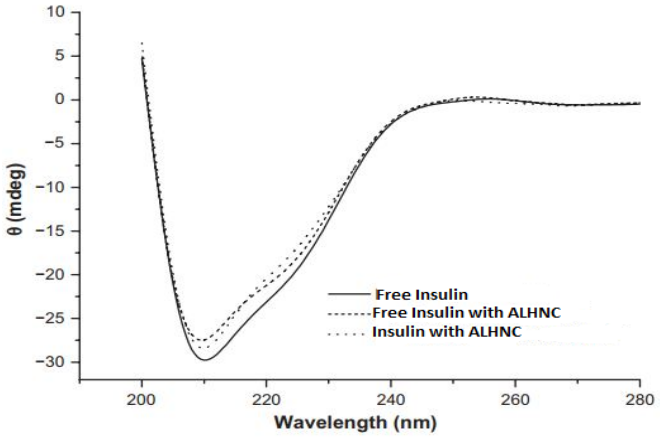

Fig. 5 Circular dichroism spectrascopy of ALHNC

Secondary structures of Ins were revealed by CD spectrascopy in Figure 5. The spectra revealed a peak-valley at about 206-208 nm and a shoulder at around 222-226 nm in both the ALHNC and the Ins solution. The secondary structures of Ins were same in all samples, with 21%–22% α-helix and 27%–29% β-folds. This secondary structural analysis confirms that the conformational integrity of Ins was preserved during the synthesis of ALHNC, both with and without Ins [17].

7.7 In vitro Drug Release

In Fig. 6 shows the results of the optimization testing of ALHNC, showing that certain lipid and polysaccharide contents produced the best loading efficiency, optimal release behavior, and full release extent. 86% of the encapsulated Ins was released in 24 hours in phosphate-buffered saline (PBS) at pH 7.4, suggesting that the optimized ALHNC produced almost all of the Ins. Ins release rates were lower in (SIF) at pH 6.8, (SGF) pH 1.2, and PBS medium pH 7.4 (20%±2.1% for burst and 78%±6.5% for total). The protonation of important carboxyl groups in alginate probably kept it in a cationic state at pH 6.8, which attracted negatively charged Ins and delayed its release. The formulation, on the other hand, showed a notable burst and full release at pH 7.4.

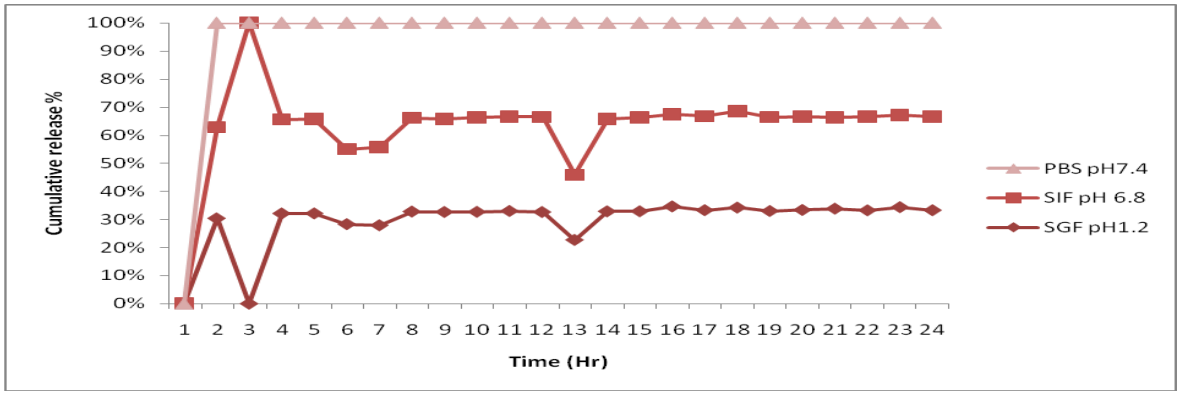

Fig. 6 Ins in vitro release profile from ALHNC in SGF (pH 1.2, 2 hr), SIF, (pH 6.8, 2 hr), and PBS buffer (pH 7.4, 2 hr).

7.8 Transepithelial Electrical Resistance (TEER) and Ins Transport Studies

Caco2 cell lines were grown at a cell density of 5×10^5 per well using transmembrane inserts with a pore size of 0.4 µm (Millipore). TEER investigations were carried out by measuring the TEER of the cell monolayer at predetermined intervals and at 37°C, according to a previously described technique shown in Fig. 7, Ins-loaded plain ALHNC with a concentration of 10 mg/mL/well was used for measurements. Also, for comparative studies, the same concentration of aspart Ins, a new short-acting human Ins analogue, was added to both plain and Ins-loaded ALHNC. Aspart Ins makes it easier to pass through the lumen epithelium because it is monomeric and has a linear structure in aqueous solutions [30].

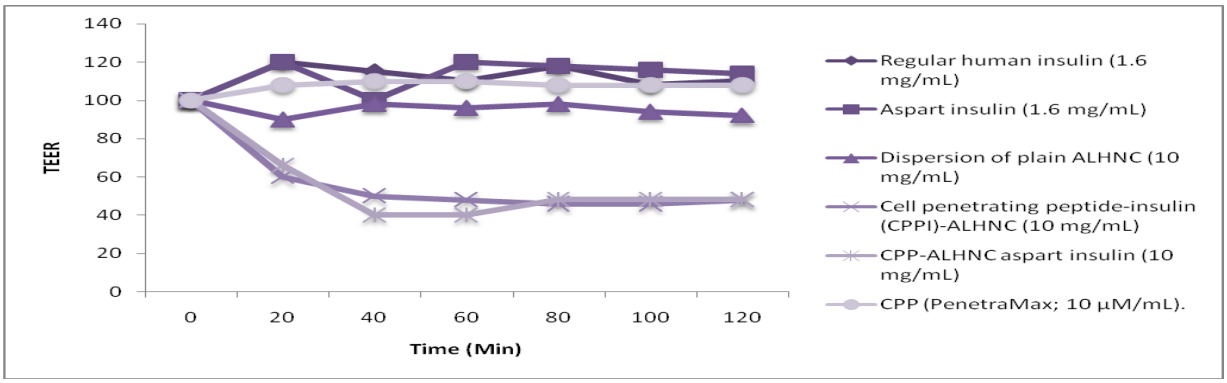

Fig. 7 Outcome of diverse formulations on TEER

We performed comparative research using human Ins and aspart Ins under the same conditions in order to assess the effectiveness of Alginate-Lipid Hybrid Nanocomposites ALHNC in comparison to aspart Ins. A control solution including both human and aspart Ins was delivered into the donor chamber of the cell layer. For Ins transport investigations, fresh media containing either plain ALHNC or ALHNC loaded with Ins (10 mg/well) was then added to the donor chamber medium. Aliquots were taken from the receiver chamber at pre-arranged intervals over the course of four hours, and a particular ELISA kit that was sensitive to both aspart and ordinary human Ins was used to measure the amount of Ins present. For every experiment conducted in triplicate, the data were averaged. The following formula was used to get Ins's apparent permeability coefficient (P_{app}):

$$P_{app}=dQ/dt_A \times C_0$$

Where dQ/d_t represents the permeability rate, A denotes the surface area of the filter membrane, and C_0 is the initial Ins concentration in the apical chamber [23,30].

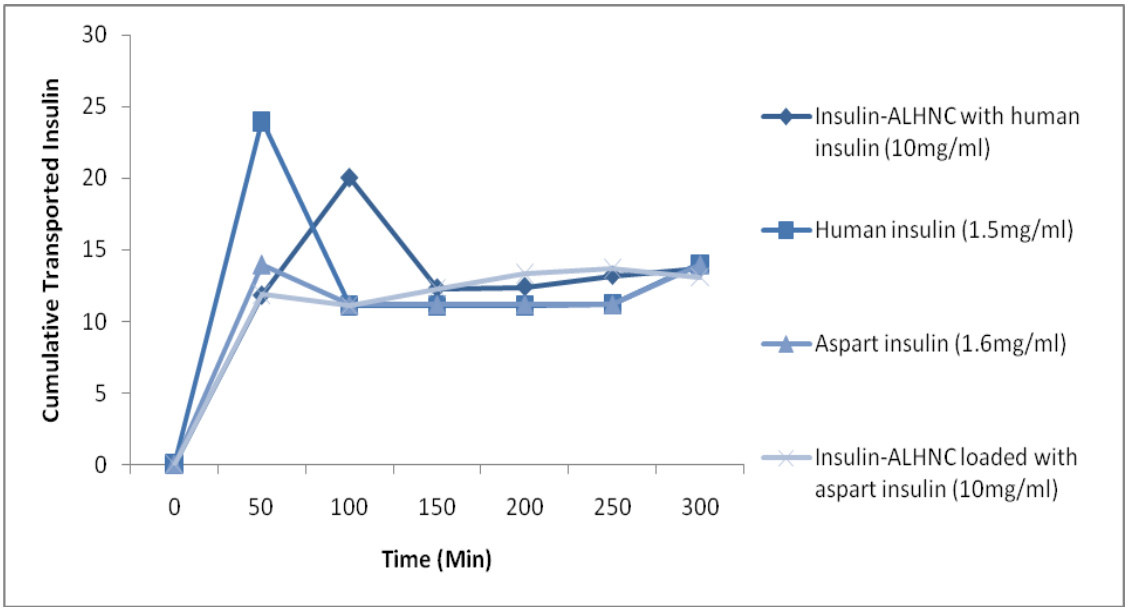

Fig. 8 Collective transported formulation of Ins

7.8 In vitro Cytotoxicity of ALHNC

In Fig. 9, cell viability was greater than 90% at doses equal to 10 μg/mL of Ins. But when Ins-loaded ALHNC concentrations increased, there was a notable decrease in cell viability ($p<0.05$), most likely as a result of the increased alginate content. Generally speaking, ALHNC's safety profile is improved by the slight positive charge that results. In the subsequent experiment, a nano composite of 10 μg/mL of both Ins and fat was used [30-33].

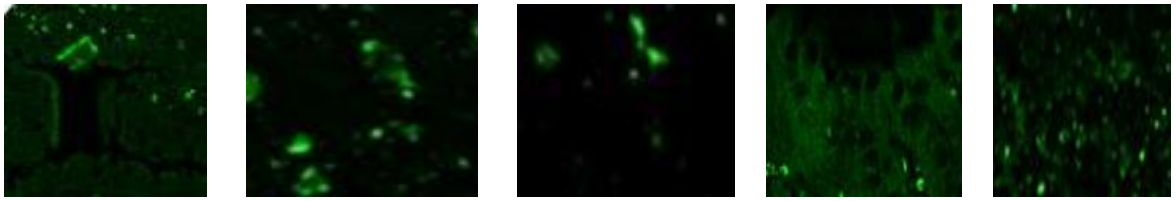

(a) (b) (c) (d) (e)

Fig. 9 Images of Light microscope as Caco-2 exposure to (a) Ins-FITC for 5 hr, ALHNC - Ins for 1,2,3,4 and 5 hours

Caco-2 cells did not glow after being incubated with Ins FITC for five hours. Probably because Ins has a large molecular weight, it hinders cellular internalization (Fig. 9). The effective internalization of Ins by the cells was demonstrated by the large number of green fluorescent spherical particles seen in CLSM micrographs of ALHNC-Ins. Further supporting increased cellular absorption of Ins, the fluorescent dye's intensity increased with longer incubation periods [30-33].

7.9 Tracking the Ins-ALHNC cellular uptake pathway

In Fig. 10 displays the experiment's results. ALHNC significantly reduced the absorption of Ins in Caco-2 cells ($p<0.05$), indicating that ALHNC-Ins can enhance the internalization of Ins. A range of chemical agents were used to pre-treat Caco-2 cells in order to determine the mechanism of ALHNC absorption. Chlorpromazine, nystatin, amiloride, and colchicine were found to cause clathrin-mediated endocytosis, caveolae-mediated endocytosis, macropinocytosis, and microtubular-mediated endocytosis, respectively. The cellular uptake of Ins nanoparticles was dramatically reduced by all inhibitors except chlorpromazine ($p>0.05$), as illustrated in Fig. 10. This suggests clathrin-mediated endocytosis is not an Ins transporter mechanism (ALHNC). On the other hand, the cholesterol-binding drug nystatin stops caveolae-mediated endocytosis by causing sag formation [20].

As previously shown, caveolae-mediated endocytosis involves separating caveolae from the plasma membrane in order to transport nanocargo to caveosomes and stop the degradative lysosomal pathway. Amiloride also inhibits necessary Na^+/H^+ exchange in the plasma membrane, a phase necessary for macropinocytosis. By binding to tubulin irreversibly and blocking microtubule polymerization, colchicine reduces microtubule-mediated endocytosis. Due to the presence of heparan sulphate proteoglycans and the negative charge of the cell membrane, microtubules typically form a cytoplasmic network that participates in the trafficking of endocytic particles. The detrimental effects of several proteoglycans found on cell membranes are lessened when they are hydrolyzed by enzymes known as heparinases. Ins cellular internalization was reduced by 80% when Caco-2 cells were pre-treated with enzymes because the cationic nanoparticles and the less negative cell membrane had less electrostatic contact. Finally, non-destructive caveolae-mediated endocytosis, which targets Vitamin B_{12} receptors, transports the particles [30-33].

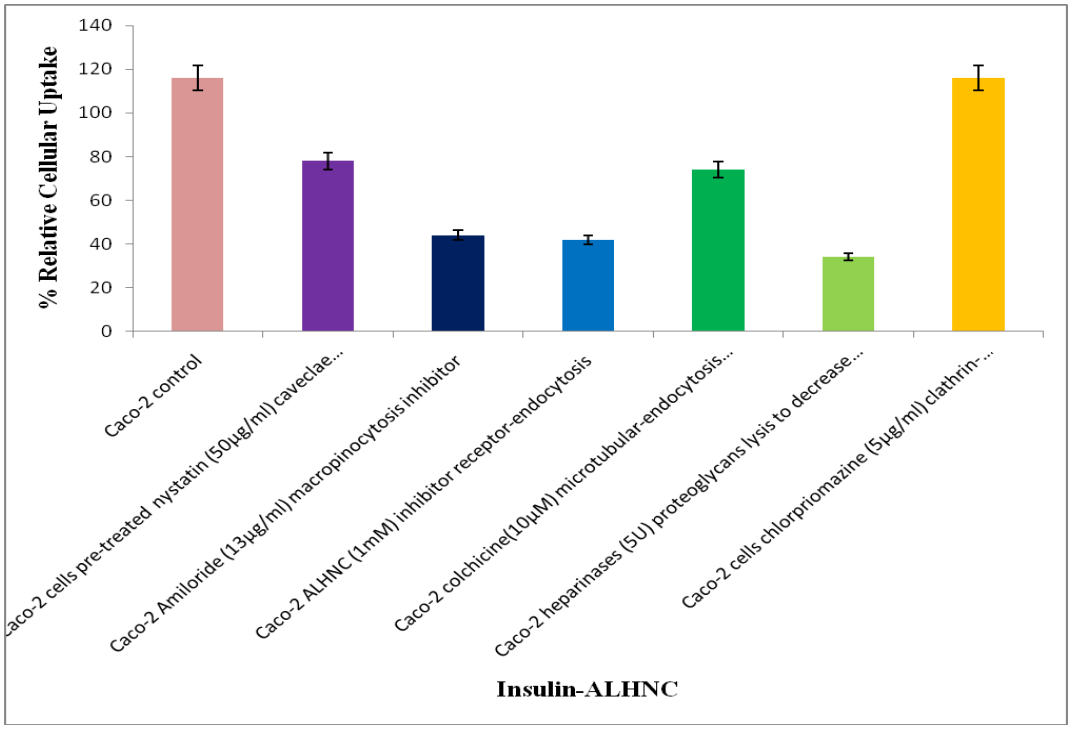

Fig. 10 The effect of various endocytosis inhibitors on Caco-2 cellular Ins uptake after incubation with ALHNC

7.10 Intestinal uptake

Histocompatibility studies demonstrated no histological changes in rat intestinal mucosa following oral administration of ALHNC-insulin. In contrast, oral administration of insulin FITC resulted in no fluorescence in the colon (Fig. 11 A,B,C) likely due to insulin's inability to traverse the intestinal walls and its rapid degradation in the gastrointestinal system. However, fluorescence was observed throughout the digestive system with ALHNC insulin, indicating its protective effect against enzymatic degradation. The ALHNC was Found on the mucosal surface, deep within muscular layers, and the submucosa. The interaction between the negatively charged cell membrane and the positively charged ALHNC allowed for mucosal retention. Additionally, ALHNC insulin was detected in Peyer's patches, where adsorptive endocytosis predominantly facilitated internalization. The ALHNC's superior properties, including mucoadhesion and enhanced penetration through the opening of tight junctions, facilitated its entry into the intestinal wall [32]. These findings align with recent research in nanotechnology, indicating both transcellular and receptor mediated endocytosis as mechanisms of cellular absorption for ALHNC-insulin [33].

After oral treatment of ALHNC-insulin, histocompatibility testing showed no histological alterations in the intestinal mucosa of rats. Conversely, when insulin FITC was administered orally, there was no fluorescence in the colon (Fig. 12 A, B, C). This is probably because insulin is unable to pass through intestinal walls and degrades quickly in the gastrointestinal tract. But with ALHNC insulin, fluorescence was seen all across the digestive tract, suggesting that it had a protective effect against enzymatic breakdown. The ALHNC was discovered on the submucosa, deep within the layers of muscles, and on the mucosal surface.

Mucosal retention was made possible by the interaction between the positively charged ALHNC and the negatively charged cell membrane. Furthermore, ALHNC insulin was found in Peyer's patches, where internalization was mostly aided by adsorptive endocytosis. The excellent qualities of ALHNC, such as improved penetration through the mucosa and mucoadhesion [30,33].

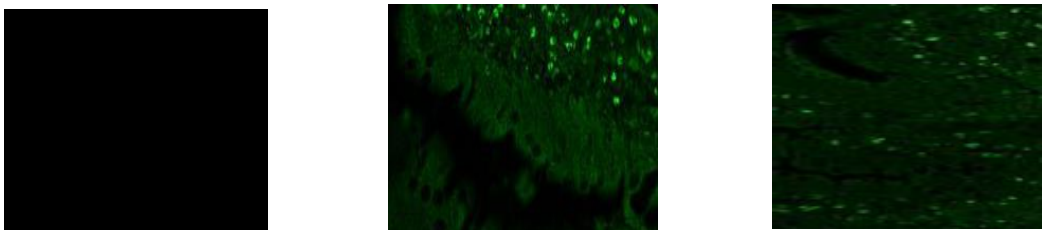

(A) (B) (C)

Figure : 12 Confocal (ALHNC) of rat intestinal mucosa and orally (A) insulin-FITC (A) and (C) ALHNC-insulin-FITC

7.11 In vivo Pharmacokinetics

A controlled investigation using two groups of six male albino rats was carried out to assess the effectiveness of insulin-loaded ALHNC. Figure 13 shows the concentration versus time relationship that was created in order to evaluate pharmacokinetic parameters. According to this study, phospholipid and polymer work together to provide a medium for regulated drug delivery and have a considerable impact on pharmacokinetic parameters [32,33]. Maximum concentration was reached in 1±0.05 hours for the medication solution group and 6±0.15 hours for the ALHNC formulation group. The ALHNC group's peak blood concentration was 4.07 mg/mL, while the medication solution group's was 1.01 mg/mL. To increase exposure and lessen the adverse effects of chemotherapeutic drugs, a lower peak concentration is thought to be advantageous. The insulin-loaded ALHNC formulation demonstrated a regulated, sustained release with a half-life of 14.0±0.4 hours, which was noticeably longer than the 1.25±0.04 hours seen in the drug solution group. Further confirming the regulated release of insulin, the mean residence time (MRT) for the lipid-polymer hybrid formulation was 20.8±0.3 hours, while the MRT for the insulin medication solution was 6.0±0.5 hours. This increase resulted from improved absorption and protection against protein binding by the lipid layer. The area under the curve (AUC) for the drug solution was 9.83±0.3 mg h/mL, whereas the AUC for the ALHNC formulation was 18.4±0.5 mg h/mL. Furthermore, the insulin volume of distribution increased by 4.6 times in the ALHNC group as opposed to 4.2 times in the insulin solution group. These findings demonstrate that the ALHNC parameters significantly improved the pharmacokinetics of insulin [26,33,]

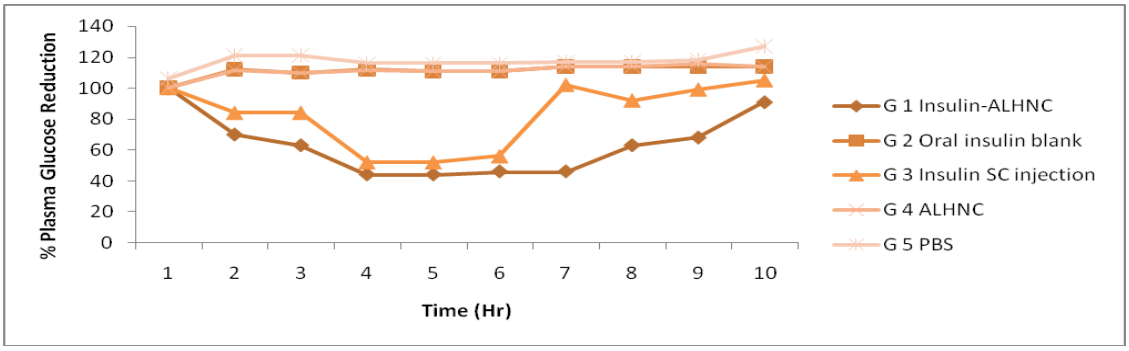

Figure12. (%) Drop in plasma glucose after treatment

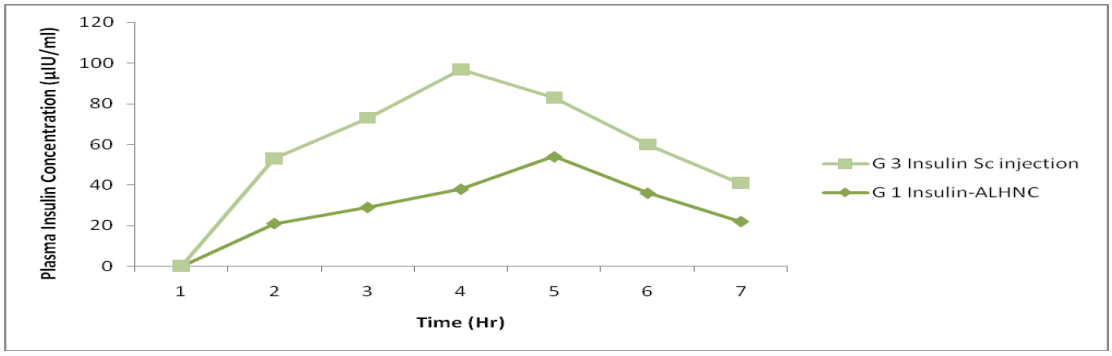

Figure13. Plasma insulin con after oral insulin ALHNC and SC insulin injection

Table 2. Pharmacodynamics of oral (ALHNC) - Sc insulin delivery

Groups	Initial plasma glucose conc. mg/dL)±SE	Pharmacodynamics parameters ± SE			
		Cmin (mg/dL)	Tmin (hr)	AUEC0-∞ (mg h/dL)	Total decrease in p.glu (%)
Group 1 received oral ALHNC-Insulin*	259.83±5.32	118.66±8.38	6hr	1690.11±3.47	32.41±2.74
Group 3 received insulin SC injection**	255.83±4.98	91.33±4.24	4hr	1814.59±3.24	27.45±2.55

Table 3. Pharmacokinetics - after oral (ALHNC) treatment, Sc insulin

Groups	Pharmacodynamics parameters ± SE				
	Cmax (µIU/mL)	Tmax (h)	AUC0-∞ (µIU h/mL)	MRT (h)	Relative bioavailability
Group 1 oral ALHNC -Insulin *	31.04±1.11	6hr	502.67±15.74	13.28±1.02	17.04%±1.34
Group 3 received Insulin Sc injection**	43.91±2.06	4hr	294.61±19.67	8.10±0.32	100

Results are the mean of six replicate±SE. *Insulin dose 50 IU/Kg. **Insulin dose 5 IU/Kg.

8. Conclusion

Synthetic Alginate Lipid Hybrid Nanocomposites ALHNC loaded with insulin have been successfully constructed in our research. These ALHNCs were carefully examined for a number of physicochemical factors, such as particle size, drug loading, entrapment efficiency, excipient compatibility, and in vitro drug release profile. With the perfect balance of lipid and alginate, the improved formulation demonstrated monodispersity, compact size, and a regulated release profile. Polymers and lipids both played important roles in the drug's release rate, which was discovered to be impacted by lowering lipid concentration. The polymer matrix and lipid layer controlled the drug's release, preventing drug leakage and guaranteeing that insulin would not burst because it was contained between the outside lipid coating and the inner polymer layer. After a 24-hour incubation period, the cytotoxic effects on Caco2 cells were validated by cell viability assays. Higher cell absorption of ALHNC was shown by additional cellular uptake investigations. Rats' regulated release pattern was shown by in vivo pharmacokinetic studies, and toxicity analyses validated ALHNC's safety profile. These results imply that ALHNCs loaded with insulin have high mucoadhesive qualities, outstanding stability, increased bioavailability, and prolonged release traits. This puts ALHNC in line with previous research as a viable nanocarrier for oral insulin administration in the management of diabetes mellitus.

Acknowledgements

We are thankful to the Management of C.Abdul Hakeem College (Autonomous), Melvisharam, Ranipet District, Tamil Nadu – India for their encouragement, providing the necessary facilities and support in carrying out the work.

Conflict of interest

Conflicts of interest all authors declare that there is no competing interest.

Reference

[1].Ong, KL; Stafford, LK, McLaughlin SA, Boyko EJ, Vollset SE, Smith AE et al (2023) Global regional and national burden of diabetes from 1990 to 2021 with projections of prevalence to 2050 a systematic analysis for the Global Burden of Disease Study 2021. J Lancet 402:203-34

[2].Maciej B , Adrianna D, Aleksandra N , Łukasz B and Bogusław O (2024) Review The Current and Promising Oral Delivery Methods for Proteinand Peptide-Based Drugs Int. J Mol Sci 25 815.

[3].Shu JC, Shuo X, Hui Ming W, Yong L, Jiahua D, Rui DX and Xiangh HS (2019) Review Articl Nanoparticles: Oral Delivery for Protein and Peptide Drugs, AAPS Pharm Sci Tech 20: 190

[4].Dhandayuthabani R, Syed Muzammil M , Sugantha Kumari V, Khaleel Basha S (2024) Studies on Choline Graft Ins Loadeded Chitosan Nanocomposite for Oral Delivery J YMER 0044-0477 Vol 23 : ISSUE 07 (7)

[5].Xin N, Zhejie C, Lan P, Lin W, Huajuan J, Yi C, Zhen Z, Chaomei F, Bo R, Jinming Z, Oral Nano Drug Delivery Systems for the Treatment of Type 2 Diabetes Mellitus: An

Available Administration Strategy for Antidiabetic Phytocompounds, International Journal of Nanomedicine 2020:15 10215–10240.
[6].Martin W, (2007) Review Article , Natural and Synthetic Polymers as Inhibitors of Drug Efflux Pumps Pharmaceutical Research, Vol. 25, No. 3, March 2008
[7]. Michał N, Maciej B , Adrianna D, Aleksandra N , Łukasz B and Bogusław O (2024) The Current and Promising Oral Delivery Methods for Proteinand Peptide-Based Drugs Int. J. Mol. Sci., 25, 815.
[8]. Shivam S, Kunal K, Shikha B C, Indu S (2023) review Emulsomes: new lipidic carriers for drug delivery with special mention to brain drug transport Future Journal of Pharmaceutical Sciences (2023) 9:78
[9]. Jiecheng Q, Yankun G, Youfa , Xinyu W Jianming C, XinW (2023) Combination of micelles and liposomes as a promising drug delivery system A Review Article Int J D Del Tra Res Pu: 06 June 2023 Volume 13, pages 2767–2789,
[10]. Khaleel Basha S, Dhandayuthabani R, Muzammil M S, Sugantha Kumari V (2020) Solid lipid nanoparticles for oral drug delivery, J Materials Today: Proceedings,.04.109
[11].Shivam S, Kunal K, Shikha B C, Indu S (2023) Emulsomes new lipidic carriers for drug delivery with special mention to brain drug transport In J Pha Sci 9:78
[12].Syed Muzammil M, Dhandayuthabani R, Sugantha Kumari V, Khaleel Basha S (2024) Probing Ins bioactivity in oral nanoemulsion produced by emulsification assisted electrostatic self assembly cross linking method An peer-revi acad Jour 0477 volume 23 : issue 02 (2)
[13].Huiwen P, Youzhi W, Yang C, Chen C, Xuqiang N, Peng L, Guojun H, Zhi P, Felicity Y H (2024) Development of polysaccharide coated layered double hydroxide nanocomposites for enhanced oral Ins delivery, In Jou D D Trans Res 14:2345–2355
[14].Weranga R, Irosha H W, Nicholas, Thoradeniya T, Nedra K D, Karunaratne V (2024) Novel alginate nanoparticles for the simulta//neous delivery of iron and folate: a potential nano-drug delivery system for anaemic patients RSC Pharm., , 1, 259–271 | 259
[15].Bialik M, Kuras M, Sobczak M, Oledzka E (2021) Achievements in thermosensitive gelling systems for rectal administration. Int J Mol Sci,22(11):5500.
[16].Fu Y, Liu P, Chen M, Jin T, Wu H, Hei M (2022) On-demand transdermal Ins delivery system for type 1 diabetes therapy with no hypoglycemia risks. J Col Interf Sci,605:582-91.
[17]. Lokesh P, Tripathy A, Yadvendra A (2017) Alginate-chitosan Coated Lecithin Core Shell Nanoparticles for Curcumin Effect of Surface Charge on Release Properties and Biological Activities I J P E R | Vol 51 | Issue 2 | Apr-Jun,
[18].Karmakar S, Bhowmik M, Laha B (2023) Recent advancements on novel approaches of Ins delivery Med Nov Technol19100253.
[19].Se Min K , Madhumita P, Rajkumar P (2021) Core-Shell Nano/ Microparticle Delivery System for Biomedical Application. J Polymers, 13, 3471.
[20].Chen Y, Song H, Huang K, Guan X (2021) Novel porous starch/ alginate hydrogel for controlled Ins release with 2 dual response of pH and amylase rsc .li Food Funct.,
[21]. Choudhury RR, Mukherjee R. (2022) Polymeric nanoparticle based oral Ins delivery system. Biomed Res; 33(2) 30-36.
[22].Nilam H P, PadmaVD (2014) Ins-loaded alginic acid nanoparticles for sublingual delivery. J Drug Deliv, Early Online: 1–8 Informa Healthcare USA, Inc.

[23]. Kannapin F, Schmitz T, Hansmann J, Schlegel N, Meir M (2021) Measurements of transepithelial electrical resistance (TEER) are affected by junctional length in immature epithelial monolayers Inter J Histoch Cell Bio 156 609–616
[24]. Gong Y, Mohd S, Wu S (2021) pH-responsive cellulose-based microspheres designed as an effective oral delivery system for Ins. ACS Omega 6(4) 2734-2741.
[25].Sandeep K, Gaurav B, Ritesh K V, Dinesh D, Neeraj D, Ki Hyun K (2016) Metformin-loaded alginate nanoparticles as an effective antidiabetic agent for controlled drug release J Ph Pharma
[26].Fengming T, Huan L, Kai Z, Lulu X 1, Dahan Zhang 1, Yang Han 2, Jing Han (2023) Sodium Alginate/Chitosan-Coated Liposomes for Oral Delivery of Hydroxy Sanshool In Vitro and In Vivo Evaluation Jour Pharm, 15
[27].Muhammad M K, Asadullah M, Vladimir T, Nina F, Jiayi P, Nayab T, Hassan S (2019) Lipid-chitosan hybrid nanoparticles for controlled delivery of cisplatin, Drug Delivery, 26:1, 765-772, 1642420
[28]. Mohanty A R, Ravikumar A, Peppas N A (2022) Recent advances in glucose-responsive Ins delivery systems novel hydrogels and future applications. Regen Biomater 9: rbac056.
[29].Muhammad A K, Chun Y, Zheng F, Shuangshuang H, Hao C, Amr M B, Li Liang, (2019) Alginate/chitosan-coated zein nanoparticles for the delivery of resveratrol, Journal of Food Engineering .04.010
[30]. Di Marzio L, Marianecci C, Cinque B, Nazzarri M, Cimini AM, Cristiano L, Cifone MG, Alhaique F, Carafa M (2011) pH-sensitive non-phospholipid vesicle and macrophage-like cells: binding, uptake and endocytotic pathway Bioch Biophys Acta 1778 2749-2756.
[31]. Zhao F, Zhao Y, Liu Y, Chang X, Chen C, Zhao Y, (2011) Review Cellular uptake, intracellular trafficking, and cytotoxicity of nanomaterials J Nano T S, 2011 May 23;7(10)1322-37.
[32].El Leithy ES, AbdelBar HM, Abd el Moneum R, Synthesis optimization and characterization of folate chitosan polymer conjugate for possible oral delivery of macromolecular drugs IOSR J. Pharm, 7 30-38.
[33].Xiao Y, Tang Z, Huang X(2021) Glucose-responsive oral Ins delivery platform for one treatment a day in diabetes. Jo of Matter 4(10) 3269-3285.